September 2001

Domain state susceptibility in FeCl2/CoPt-heterostructures

Christian Binek
University of Nebraska-Lincoln, cbinek@unl.edu

phys. stat. sol. (a) **189**, No. 2, 575–583 (2002)

Domain State Susceptibility in $FeCl_2$/CoPt Heterostructures

CH. BINEK[1]), A. HOCHSTRAT, and W. KLEEMANN

Laboratorium für Angewandte Physik, Gerhard-Mercator-Universität, Lotharstr. 1, D-47048 Duisburg, Germany

(Received May 1, 2001; accepted September 30, 2001)

Subject classification: 75.50.Ee; 75.60.Ch; 75.70.Cn; S1.1; S1.2

Magnetic heterostructures with perpendicular anisotropy consisting of antiferromagnetic (111)-oriented $FeCl_2$ single crystals and thin ferromagnetic CoPt-multilayers are investigated by ac-susceptometry after cooling in various axial magnetic fields to below the Néel temperature. The freezing process drives the system into a metastable antiferromagnetic domain state which gives rise to a huge excess contribution to the complex parallel susceptibility on heating in zero magnetic field. Its glow curve-like temperature dependence is modeled within the framework of a simple analytical approach. It involves the susceptibility of thermally activated clusters originating from antiferromagnetic stacking faults as well as the contribution of pairs of antiparallel Ising spins which build up walls within the ferromagnetically ordered (111) planes.

1. Introduction Heterostructures which combine antiferromagnetic (AF) and ferromagnetic (FM) materials exhibit the effect of exchange biasing, which is one of the most challenging topics in modern thin film magnetism. It describes a coupling phenomenon between the FM and AF materials which is phenomenologically characterized by a shift of the ferromagnetic hysteresis loop along the magnetic field axis [1–3]. This shift reflects an unidirectional anisotropy which originates from the interface coupling of the ferromagnet and its AF pinning layer. The particular interest in this effect originates on the one hand from its huge technological potential in passive spin electronic devices [4]. On the other hand, the microscopic details of the exchange bias mechanism are still under debate [5]. This situation triggers an abundance of basic research activities [6–15]. The understanding of the phenomenon on a microscopic level needs detailed insight into the complex thermal and field-dependent evolution of the spin-structure of the heterosystem [16, 17]. It establishes on freezing the AF pinning layer to below its Néel temperature. In addition, during a magnetization reversal process of the exchange coupled ferromagnet a further and partly irreversible evolution of the AF spin structure takes place [18, 19].

In order to tackle this complex problem, model systems are required, which exhibit the basic mechanisms of the exchange bias effect in a very pronounced way. Heterolayer structures of perpendicular anisotropic antiferro- and ferromagnets involve a limited number of spin degrees of freedom. This minimized complexity of possible spin arrangements gives rise to model type behavior of such heterosystems [20, 21].

$FeCl_2(111)/\{Co\ 0.35\,nm/Pt\ 1.2\,nm\}_{10}/Pt\ 0.8\,nm$ reflects such a prototypical system where excessive AF domain growth and evolution can be studied. The $CdCl_2$-type structure of the rhombohedral $FeCl_2$ single crystal builds up a lattice of space group symmetry D^5_{3d} [22]. Hexagonal layers of ferromagnetically coupled Fe^{2+} ions are sepa-

[1]) Corresponding author; Fax: +49-203-379-1965; e-mail: binek@kleemann.uni-duisburg.de

 0031-8965/02/18902-0575 $ 17.50+.50/0

rated by two layers of Cl^- and experience a weak antiferromagnetic interlayer ordering. The Fe^{2+} ions carry effective spins of $S = 1$. The large crystal field induced single ion anisotropy gives rise to the strong Ising-character of the system. An uncompensated (111) layer of $FeCl_2$ builds up the interface with the adjacent CoPt multilayer of perpendicular anisotropy.

In contrast with the prototypical antiferromagnet FeF_2, moderate axial magnetic fields of $\mu_0 H \approx 1$ T give rise to a metamagnetic transition in $FeCl_2$ [23–25]. It takes place below the tricritical temperature $T_t = 21.7$ K where the system flips from the AF into a paramagnetic saturated state. Moreover, $FeCl_2$ exhibits a zero-field susceptibility at the Néel temperature $T_N = 23.7$ K, which is huge in comparison with the parallel susceptibility of, e.g., FeF_2. We believe that this difference subdivides the perpendicular anisotropic systems into two classes. As is well known [5], the "hard" antiferromagnet FeF_2 pins the FM top layer on cooling to below the Néel temperature. Contrastingly we shall show in the present paper that in heterostructures based on the "soft" antiferromagnet $FeCl_2$ the long-range ordered AF state breaks into a metastable domain state on field cooling. This domain state is highly susceptible to axial magnetic fields. Moreover, upon heating towards T_N it exhibits a thermally activated relaxation towards the AF long-range ordered ground state.

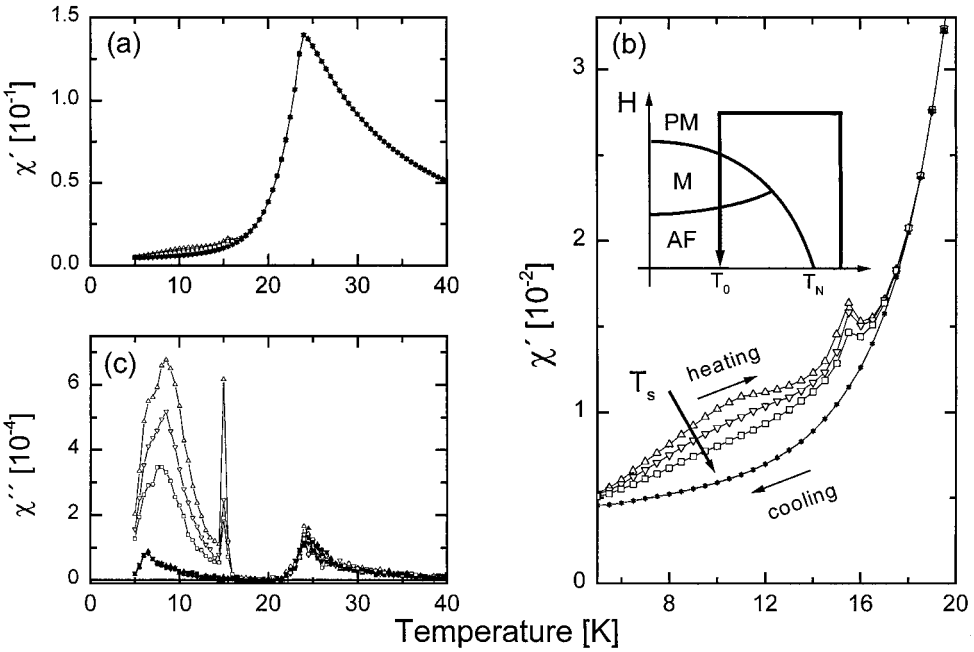

Fig. 1. Temperature dependence of the a) real and c) imaginary part of the ac-susceptibility $\chi = \chi' - i\chi''$ of $FeCl_2$(111)/{Co 0.35 nm/Pt 1.2 nm}$_{10}$/Pt 0.8 nm at frequency $f = 10$ Hz. Schematic phase diagram of $FeCl_2$ (inset of b)) shows the preparation of the initial state. After freezing in an axial field of $\mu_0 H = 5$ T down to $T_0 = 11$ (up triangles), 12 (down triangles) and 13 K (squares), the field is rapidly decreased towards zero and χ' (a) and b) open symbols) and χ'' versus T (c) open symbols) is measured for $T_s = 5$ K $< T <$ 40 K to above $T_N = 23.7$ K. Solid symbols show χ' (parts a and b) and χ'' versus T (part c) versus T, respectively

2. Experimental Results In Fig. 1a we present the temperature dependence of the ac-susceptibility $\chi = \chi' - i\chi''$ of a $FeCl_2(111)/\{Co\ 0.35\ nm/Pt\ 1.2\ nm\}_{10}/Pt\ 0.8\ nm$ multilayer as measured by SQUID-susceptometry at the frequency $f = 10$ Hz. The preparation of the initial state of the sample is schematically shown in the magnetic phase diagram of $FeCl_2$ as depicted in the inset of Fig. 1b. H designates the magnetic field applied perpendicularly to the (111) cleavage plane. It gives rise to isothermal metamagnetic AF-to-paramagnetic (PM) phase transitions below T_N, involving a mixed phase (M) along the low-T first-order phase line. After cooling in an axial freezing field of $\mu_0 H = 5$ T down to $T_0 = 11$ (up triangles), 12 (down triangles) and 13 K (squares), the field is rapidly decreased towards zero where the AF order of the pinning layer becomes frozen-in. On subsequent heating, both χ' and χ'' versus T exhibit pronounced excess contributions showing a broad and a narrow peak at $T \approx 12$ and ≈ 15 K, respectively. They vanish on subsequent zero-field cooling from $T = 40$ K back to $T = 5$ K, i.e. to far below the Néel temperature $T_N = 23.7$ K of $FeCl_2$ (see details of χ' versus T in Fig. 1b).

3. Model and Analysis Figure 2 shows a sketch of the spin structure of a $FeCl_2$/CoPt heterolayer growing at a single-atomic step of the as-cleft $FeCl_2$ single crystal. Such a structure is expected on cooling to below the Néel temperature in an axial magnetic field that aligns the FM moments, but is small in comparison with the exchange field between the AF and FM spins at the interface. In that case, the interface coupling (assumed to be AF in Fig. 2) controls the preferred orientation of the AF moments at the interface. Its roughness prevents the evolution of long-range AF order and gives rise to the formation of AF domains. They start to grow at the interface and end up in the AF bulk.

Note, that a similar domain state is expected when $FeCl_2$ without a FM top layer is isothermally demagnetized from the saturated PM into the AF state across the spin-flip transition (inset Fig. 1b). In that case, the axial magnetic field at the spin-flip transition aligns the moments of the uncompensated (111)-surface parallel to the c-axis. These spins are particularly affected by the field owing to the reduced superexchange interaction which surface moments experience with respect to the bulk moments of the antiferromagnet. Hence, in the case of $FeCl_2$ single crystals the applied field corresponds to the exchange field at the AF/FM interface of the $FeCl_2$/CoPt hetrostructure. The latter one, however, is supposed to exceed the applied field when the spin-flip transition takes place in a heterostructure in the presence of exchange at the interface. Analogously to the situation shown in Fig. 2 the field-aligned uppermost layer at the rough surface is the starting point for AF domain formation.

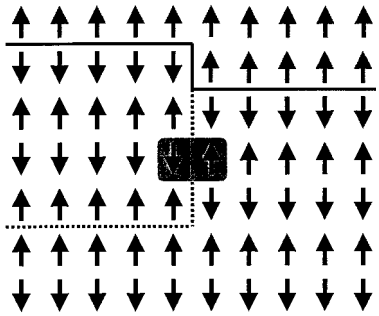

Fig. 2. Sketch of the spin structure of an $FeCl_2$/CoPt heterostructure after freezing in an axial magnetic field that polarizes the FM moments (uppermost layers). The solid line represents the AF/FM interface. Interface roughness drives the AF bulk via exchange interaction into the domain state. Pairs of spins (gray background) build up the vertical domain wall (vertical dashed line). AF stacking faults give rise to a horizontal domain wall perpendicular to the c-axis (horizontal dashed line)

Figure 2 exhibits two types of domain walls. On the one hand, the 2D FM order within the (111)-planes is broken. The basic elements of these "vertical" domain walls are pairs of antiparallel aligned spins (see the gray highlighted spin pair in Fig. 2). They enhance the magnetic energy by the individual amount of $+2J$ each, where $J > 0$ is the intraplanar FM exchange constant. On the other hand, AF stacking faults give rise to "horizontal" AF domain walls which break the symmetry along the *c*-axis and, hence, carry a net magnetic moment when forming under an aligning external field [26]. Both types of domain walls correspond to distinct susceptibility contributions and will be discussed subsequently.

We start with the contribution of the spin pairs within the vertical walls. Each pair gives rise to a susceptibility contribution which is determined by the energies of the four spin configurations of the two Ising spins. Assuming that the AF ordered neighborhood of a given spin pair remains virtually unchanged in the temperature range $5\,\mathrm{K} < T < 20\,\mathrm{K}$ where the excess susceptibility evolves, the four energy values

$$E_j = K_j - g\mu_B\mu_0 H S_j^{\mathrm{tot}} \tag{1}$$

describe the equilibrium thermodynamic behavior of the spins. K_j summarizes the exchange interaction energy between the spins of a given pair and all the surrounding spins that interact with the pair via exchange. The second term takes into account the Zeeman energy of the two spins in the applied magnetic field. The index j labels one out of the four configurations which correspond to the total spin values $S_j^{\mathrm{tot}} = \pm 2$ in the case of parallel spin alignment ($j = 0$ and 1) while the two spin configurations of antiparallel alignment yield $S_j^{\mathrm{tot}} = 0$ ($j = 2$ and 3). Each spin pair is assumed to give rise to the same susceptibility contribution. The total susceptibility is then calculated from the total free energy expression of the spin pairs,

$$F_{\mathrm{sp}} = -k_B T N \ln\left(\sum_{j=0}^{3} \mathrm{e}^{-E_j/(k_B T)}\right), \tag{2}$$

where N is the number of spin pairs building up the AF domain walls. The static magnetic susceptibility in zero external field, $H = 0$, is calculated according to

$$\chi_{\mathrm{sp}} = -\left(\frac{\partial^2 F_{\mathrm{sp}}}{\partial H^2}\right)_{H=0} = C\beta\, \frac{\mathrm{e}^{\beta(\tilde{K}_1+\tilde{K}_2+\tilde{K}_3)}\left(4\mathrm{e}^{\beta\tilde{K}_1} + \mathrm{e}^{\beta\tilde{K}_2} + \mathrm{e}^{\beta(\tilde{K}_1+\tilde{K}_2)} + \mathrm{e}^{\beta\tilde{K}_3} + \mathrm{e}^{\beta(\tilde{K}_1+\tilde{K}_3)}\right)}{\left(\mathrm{e}^{\beta(\tilde{K}_1+\tilde{K}_2)} + \mathrm{e}^{\beta(\tilde{K}_1+\tilde{K}_3)} + \mathrm{e}^{\beta(\tilde{K}_2+\tilde{K}_3)} + \mathrm{e}^{\beta(\tilde{K}_1+\tilde{K}_2+\tilde{K}_3)}\right)^2}. \tag{3}$$

where $\tilde{K}_j = K_j - K_0$, $\beta = 1/(k_B T)$ and $C{=}N(2g\mu_B\mu_0)^2$. On a mesoscopic scale, each domain wall separates two regions which are related by time inversion (see Fig. 2). Hence, the two configurations with $S_{j=0,1}^{\mathrm{tot}} = \pm 2$ possess identical exchange energies, i.e. $K_0 = K_1$. Let $j = 3$ label the spin configuration with $S_{j=3}^{\mathrm{tot}} = 0$ where both spins of the pair are flipped with respect of the configuration $j = 2$ which is shown in Fig. 2. In that case, $j = 3$ represents the energetically most unfavorable state. Hence, it is reasonable to assume, that its thermal excitation is negligible in comparison with the population of the states $j = 0$, 1, 2. Therefore, the susceptibility is determined by the single energy parameter $\tilde{K}_2$, the difference between the exchange energy of the $S_{j=0,1}^{\mathrm{tot}} = \pm 2$ and $S_{j=2}^{\mathrm{tot}} = 0$ configuration. The simplified expression (3) reads

$$\chi_{\mathrm{sp}} = \frac{2C\beta}{2 + \mathrm{e}^{\beta\tilde{K}_2}}. \tag{4}$$

The domain structure is a metastable state which relaxes into the AF long-range ordered state. Its relaxation time is long in comparison with the inverse ac-frequency of the measurement $\tau = 1/\nu = 0.1$ s. Therefore, the relaxation affects the susceptibility only by the reduction of the number of spin pairs which enter Eq. (4) via C. The expected decay rate, $\mathrm{d}N/\mathrm{d}t$, of the spin pairs is given by

$$\frac{\mathrm{d}N}{\mathrm{d}t} = -\alpha(T)\, N\,, \tag{5}$$

where a decay constant with Arrhenius-type thermal activation,

$$\alpha = \alpha_0\, \mathrm{e}^{-\Delta E/(k_\mathrm{B}T)} \tag{6}$$

is assumed for temperatures well below T_N. Here ΔE is the energy barrier and α_0 is a phenomenological attempt frequency. The ac-susceptibility is measured by Superconducting Quantum Interference Device technique (SQUID Quantum Design MPMS5S) after thermal stabilization of each temperature value of the subsequent data points. Thermal stabilization and measurement require an average time interval of $\Delta t \approx 124$ s. In the case of temperature steps of $\Delta T = 1$ K this yields the average heating rate $q = \Delta T/\Delta t \approx 8$ mK/s and a corresponding linear temporal increase of the temperature

$$T(t) = q(t - t_0) + T_\mathrm{s}\,. \tag{7}$$

Here t_0 and T_s are the time and the temperature at the start of the measurement, respectively. In accordance with Eq. (7), the time dependence of the temperature affects the solution of Eq. (6). Integration yields

$$N(T) = N_0\, \mathrm{e}^{-\frac{1}{q}\int_{T_\mathrm{s}}^{T} \alpha(T')\,\mathrm{d}T'}\,, \tag{8}$$

the temperature dependent number of spin pairs which contribute to the total susceptibility of Eq. (5). Here N_0 is the total number of spin pairs which are generated during the field cooling procedure. Equation (8) is related to the Randall-Wilkins equation, which is known from the physics of thermoluminescence where trapped electrons are thermally activated and give rise to light emission on heating [27, 28]. The temperature dependence of the luminescence is also known as the "glow-curve".

In order to obtain an analytic susceptibility expression which is appropriate for a fitting procedure, the integration which enters Eq. (8) is approximately solved. Therefore, we expand $\alpha(T')$ into powers of $(T' - T^*)$ up to the first order, where $T^* = (T_\mathrm{s} + T)/2$ is the center of the integration interval. Subsequent integration with respect to T' yields

$$\int_{T_\mathrm{S}}^{T} \alpha(T')\,\mathrm{d}T' \approx \alpha(T^*)\,(T - T_\mathrm{s}) = \alpha_0\, \mathrm{e}^{-2\Delta E/(k_\mathrm{B}(T+T_\mathrm{S}))}\,(T - T_\mathrm{s})\,. \tag{9}$$

Substitution of the approximation (9) into Eq. (8) yields an explicit expression of the number of spin pairs at a given temperature T. This expression enters Eq. (4) via the proportionality constant C.

The horizontal domain walls (Fig. 2) carry an excess moment m_c which is expected to vanish as a consequence of domain relaxation. This is indeed observed, as shown in Fig. 3, which exhibits the temporal relaxation, m versus t of the magnetic moment of a

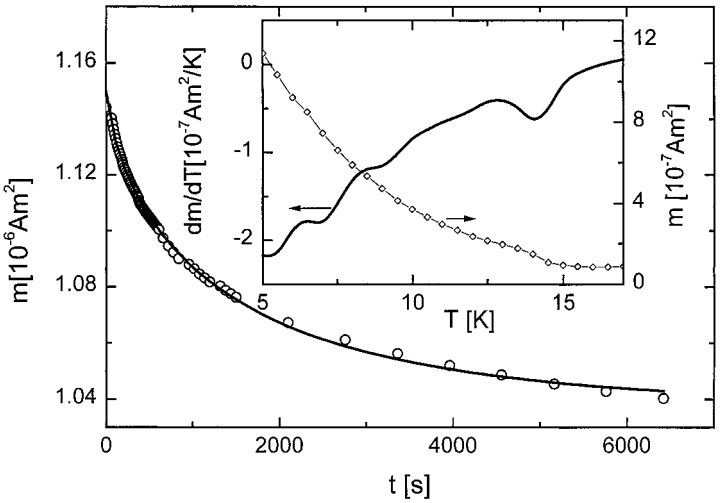

Fig. 3. Temporal relaxation of the magnetic moment (circles) at $T = 5$ K after cooling in an axial field $\mu_0 H = 5$ T. The inset shows the temperature dependence of the magnetic moment (diamonds) and its derivative (line) after the same field cooling procedure and subsequent zero-field heating

$FeCl_2$/CoPt multilayer after field cooling in $\mu_0 H = 5$ T to $T = 5$ K. A best fit to a stretched exponential function

$$m(t) = m_0 + m_1 \, \mathrm{e}^{-(t/\tau)^{\beta}} \tag{10}$$

yields $m_0 = 1.12 \times 10^{-7}$ Am^2, $m_1 = 1.1 \times 10^{-8}$ Am^2, $\tau = 1350$ s and $\beta = 0.69$. The stretched exponential decay implies a polydispersive relaxation process. Its average relaxation time is given by $\langle\tau\rangle = \tau\Gamma(1/\beta)/\beta$ [29]. With $\Gamma(1/0.69) = 0.8857$ we obtain $\langle\tau\rangle = 1733$ s. It may be considered as the typical relaxation time of the above described metastable spin configurations, which enters the domain dynamics to be discussed below.

In close analogy to the domain wall relaxation described above, it is reasonable to assume that one dominating activation energy $\Delta\tilde{E}$ controls the temporal decay of the magnetic moment. This is corroborated in the inset of Fig. 3, which shows the "glow-curve" m versus T and its derivative $\mathrm{d}m/\mathrm{d}T$ versus T. The latter one exhibits a pronounced minimum at $T = 15$ K which indicates a thermal activated relaxation towards the low moment ground state. The horizontal domain walls carry a typical magnetic moment m_c, which build up the total surplus moment of the AF bulk. In order to rotate the spins of a cluster coherently, they have to overcome the barrier $\Delta\tilde{E}$. It is expected to depend on the applied magnetic field, δH, in accordance with the Zeeman energy $\delta E = -\mu_0 m_c \delta H$. Hence, δH modifies the activation energy of each cluster by δE which gives rise to a field-dependent relaxation rate. A positive magnetic field lowers the energy of the magnetic moments which point along the field direction. Hence, the energy barrier increases with increasing magnetic field. This causes a field induced surplus magnetization with respect to the zero or negative magnetic field condition, where the reduction of the energy barrier accelerates the decay of the magnetization. This mechanism gives rise to a positive susceptibility contribution χ_c which superimposes with χ_{sp}.

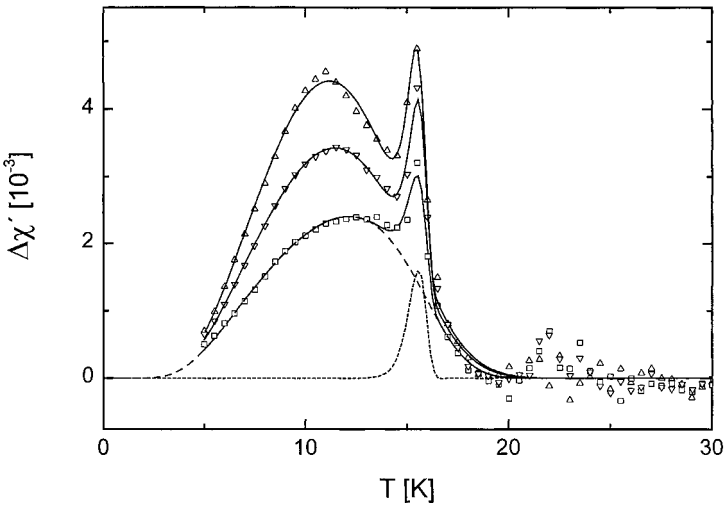

Fig. 4. Excess susceptibility $\Delta\chi$ versus T obtained from Fig. 1b after subtraction of the zero-field cooled curves using the same symbols as in Fig. 1b. The solid lines exhibit the results of best fits of $\Delta\chi(T) = \chi_{sp}(T) + \chi_c(T)$, Eqs. (4) and (12), to the data. As an example, the decomposition of $\Delta\chi$ into χ_{sp} and χ_c is shown for $T = 13$ K (dashed lines)

The relaxation of m originates from the rearrangement of energetically unfavorable oriented spins towards the magnetized ground state. In a first approximation the flipping rate of the spins can be described by Eq. (6), where the new activation energy and a new attempt frequency $\tilde{\alpha}_0$ enter $\tilde{\alpha}(T)$. The thermal evolution of the number of unfavorable oriented spins is again given by Eq. (8) by taking into account the new parameters $\tilde{\alpha}_0$ and $\Delta\tilde{E}$. It is transformed into an approximate analytic expression with the help of Eq. (9) which yields

$$m(T) = m_0 \exp\left(-\frac{\tilde{\alpha}_0(T - T_s)}{q}\, e^{-2(\Delta\tilde{E}+\mu_0 m_c H)/(k_B(T+T_s))}\right). \tag{11}$$

The derivative $\partial m/\partial H$ of Eq. (11) at $H = 0$ yields the susceptibility contribution

$$\chi_c = \frac{2\mu_0 m_0 m_c \tilde{\alpha}_0(T - T_s)}{q k_B(T + T_s)} \exp\left(-\frac{\tilde{\alpha}_0(T - T_s)}{q}\, e^{-2\Delta\tilde{E}/(k_B(T+T_s))} - \frac{2\Delta\tilde{E}}{k_B(T + T_s)}\right). \tag{12}$$

The total susceptibility is given by the sum of the spin pair and the cluster contribution. Figure 4 shows the results of best fits of $\chi(T) = \chi_{sp} + \chi_c$ to the data of the excess susceptibility obtained after subtraction of the zero-field cooled background signal (Fig. 1b).

4. Results and Discussion Here we are going to discuss the seven fitting parameters which enter our model theory to fit the experimental data of the excess susceptibility. The proportionality constant C, which enters the spin pair contribution decreases linearly from $C = 0.00144$, 0.00091 to 0.0006 for $T_0 = 11$, 12 and 13 K, respectively. It indicates that the number of wall spins increases with decreasing transition temperature

T_0, where the antiferromagnetic ordering sets in (see inset of Fig. 1b). As expected, the energy parameter $\tilde{K}_2$ which enters Eq. (4) is virtually independent of temperature and given by $\tilde{K}_2/k_B = (25.6 \pm 1.2)$ K. This is reasonable, because $\tilde{K}_2$ is determined by the microscopic exchange between the spins of a given pair and their corresponding AF ordered neighborhood. The typical interaction energy of a spin is of the order of k_B times the Néel temperature $T_N = 23.7$ K of the antiferromagnet, which is in fact pretty close to the resulting fitting parameter.

In contrast to that, the energy barrier ΔE as well as the ratio of the attempt frequency α_0 and the heating rate q increase from $\Delta E/k_B = 61.2, 79.7$ to 105.0 K and $\alpha_0/q = 44.0, 208.9$ to 1719.9 K^{-1} with increasing $T_c(H)$, respectively. The height ΔE of the barrier is given by the energy which is required in order to move two adjacent walls until they meet and annihilate each other. Hence, ΔE increases with the typical domain size. The latter one is expected to increase with increasing $T_c(H)$, because small deviations from the AF ground state are efficiently quenched by thermal spin-flips which increase with increasing temperature.

The domain walls which are generated by AF stacking faults can be regarded as FM clusters. Their contributions are given by Eq. (12). Its fit to the data yields $\Delta\tilde{E}/k_B =$ 502.5, 485.4 and 503.7 K as well as $\tilde{\alpha}_0/q = 1.7 \times 10^{20}$, 2.7×10^{19} and 1.7×10^{20} K^{-1}. The parameters are virtually temperature independent indicating that the cluster size does not depend on temperature. In order to reduce the number of these domains, coherent rotation of large regions within the FM layers is necessary, which may explain the high value of the energy barrier. Moreover, in comparison with α_0 the very high values of the attempt frequency $\tilde{\alpha}_0$ indicate that the cluster excitations are given by collective modes of the spin wave type. In contrast to the proportionality constant C, the pre-factor $P = 2\mu_0 m_0 m_c \tilde{\alpha}_0/(qk_B)$ of χ_c reveals remarkable high values of $P = 5.5 \times 10^{16}$, 7.4×10^{15} and 3×10^{16}. This is in accordance with the model assumption of AF stacking faults that carry large magnetic moments.

5. Conclusion The temperature dependence of the freezing field induced low frequency excess susceptibility of the $FeCl_2(111)$/{Co 0.35 nm/Pt 1.2 nm}$_{10}$/Pt 0.8 nm heterostructure is studied by SQUID-susceptometry. The excess with respect to the parallel zero-field susceptibility of the long-range ordered antiferromagnet is interpreted in terms of metastable AF domains which grow during the field cooling process. The perpendicular anisotropic FM polarized CoPt layer couples with the AF spins at the uncompensated rough interface of the (111)-oriented $FeCl_2$ single crystal. Hence, the topological roughness gives rise to magnetic roughness at the interface where the growth of the AF domains sets in. The experimental excess susceptibility is modeled within the framework of a phenomenological description involving spin pairs of vertical domain walls and cluster contributions of AF stacking faults. The intensity of both contributions are controlled by thermal activation processes in accordance with the metastability of the AF domain state. The description is in close analogy with the analysis of glow-curves which are known from thermoluminescence [27, 28]. The experimental results insistently demonstrate, that AF domain formation plays a crucial role in exchange bias systems where, on the one hand, pinning of the ferromagnet has to be considered, but, on the other hand, the AF/FM interaction strongly influences the AF order.

Acknowledgements The authors like to thank B. Kagerer and M. Aderholz for scientific and technical support, respectively. The work is supported by Deutsche Forschungsgemeinschaft through Sonderfoschungsbereich 491.

References

[1] W. H. Meiklejohn and C. P. Bean, Phys. Rev. **105**, 904 (1956).
W. H. Meiklejohn, J. Appl. Phys. **33**, 1328 (1962).
[2] D. Mauri, E. Kay, D. Scholl, and J. K. Howard, J. Appl. Phys. **62**, 2929 (1987).
[3] A. P. Malozemoff, Phys. Rev. B **37**, 7673 (1988).
[4] G. Prinz and K. Hathaway, Phys. Today **4**, 24 (1995).
[5] J. Nogués and I. K. Schuller, J. Magn. Magn. Mater. **192**, 203 (1999).
[6] N. C. Koon, Phys. Rev. Lett. **78**, 4865 (1996).
[7] R. Jungblut, R. Coehoorn, M. T. Johnson, J. van de Stegge, and R. Reinders, J. Appl. Phys. **75**, 6659 (1994).
[8] X. W. Wu and C. L. Chien, Phys. Rev. Lett. **81**, 2795 (1998).
[9] S. Riedling, M. Bauer, C. Mathieu, B. Hillebrands, R. Jungblut, J. Kohlhepp, and R. Reinders, J. Appl. Phys. **85**, 6648 (1999).
[10] J. Nogués, T. J. Moran, D. Lederman, and I. K. Schuller, Phys. Rev. B **59**, 6984 (1999).
[11] P. Milteni, M. Gierlings, J. Keller, B. Beschoten, G. Güntherodt, U. Nowak, and K. D. Usadel, Phys. Rev. Lett. **84**, 4424 (2000).
[12] Joo-Von Kim, R. L. Stamps, B. V. Mc Grath, and R. E. Camley, Phys. Rev. B **61**, 8888 (2000).
[13] H. Xi and R. M. White, Phys. Rev. B **61**, 80 (2000).
[14] R. L. Stamps, J. Phys. D **33**, R247 (2000).
[15] U. Nowak, A. Misra, and K. D. Usadel, J. Appl. Phys. **89**, 7269 (2001).
[16] F. U. Hillebrecht, H. Ohldag, N. B. Weber, C. Bethke, and U. Mick, Phys. Rev. Lett. **86**, 3419 (2001).
[17] H. Ohldag, A. Scholl, F. Nolting, S. Anders, F. U. Hillebrecht, and J. Stöhr, Phys. Rev. Lett. **86**, 2878 (2001).
[18] A. M. Goodman, H. Laidler, K. O'Grady, N. W. Owen, and A. K. Petford-Long, J. Appl. Phys. **87**, 6409 (2000).
[19] X. Portier, A. K. Petford-Long, and A. de Morias, J. Appl. Phys. **87**, 6412 (2000).
[20] B. Kagerer, Ch. Binek, and W. Kleemann, J. Magn. Magn. Mater. **217**, 139 (2000).
[21] Ch. Binek, B. Kagerer, S. Kainz, and W. Kleemann, J. Magn. Magn. Mater., **226–230**, 1814 (2001).
[22] J. C. Slater, Quantum Theory of Molecules and Solids, Vol. 2, McGraw-Hill Book Co., New York 1965 (p. 77 ff.).
[23] L. J. De Jongh and A. R. Miedema, Adv. Phys. **23**, 1 (1974).
[24] R. Birgeneau, W. B. Yelon, E. Cohen, and J. Makovsky, Phys. Rev. B **5**, 2607 (1972).
[25] J. F. Dillon, E. Y. Chen, and H. J. Guggenheim, Phys. Rev. B **18**, 377 (1978).
[26] N. Papanicolaou, Phys. Rev. B **51**, 15062 (1995).
[27] J. T. Randall and M. H. F. Wilkins, Proc. R. Soc. Lond. A **184**, 347 (1945);
Proc. R. Soc. Lond. A **184**, 364 (1945);
Proc. R. Soc. Lond. A **184**, 391 (1945).
[28] G. F. Garlick and M. H. F. Wilkins, Proc. R. Soc. Lond. A **184**, 408 (1945).
[29] K. Binder and J. D. Reger, Adv. Phys. **41**, 547 (1992).